

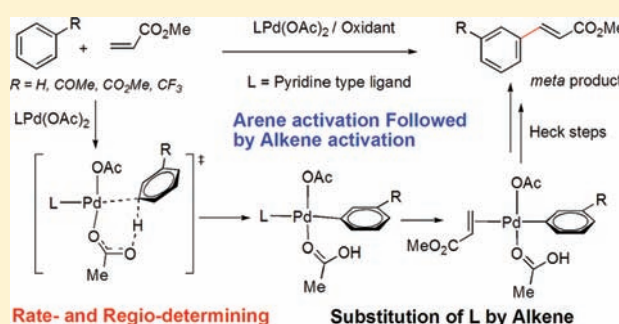
# Theoretical Analysis of the Mechanism of Palladium(II) Acetate-Catalyzed Oxidative Heck Coupling of Electron-Deficient Arenes with Alkenes: Effects of the Pyridine-Type Ancillary Ligand and Origins of the *meta*-Regioselectivity

Songlin Zhang,\* Li Shi, and Yuqiang Ding

School of Chemical and Material Engineering, Jiangnan University, Wuxi 214122, Jiangsu Province, China

Supporting Information

**ABSTRACT:** A systematic theoretical study is carried out on the mechanism for Pd(II)-catalyzed oxidative cross-coupling between electron-deficient arenes and alkenes. Two types of reaction pathways involving either a sequence of initial arene C–H activation followed by alkene activation, or the reverse sequence of initial alkene C–H activation followed by arene activation are evaluated. Several types of C–H activation mechanisms are discussed including oxidative addition,  $\sigma$ -bond metathesis, concerted metalation/deprotonation, and Heck-type alkene insertion. It is proposed that the most favored reaction pathway should involve an initial concerted metalation/deprotonation step for arene C–H activation by (L)Pd(OAc)<sub>2</sub> (L denotes pyridine type ancillary ligand) to generate a (L)(HOAc)Pd(II)–aryl intermediate, followed by substitution of the ancillary pyridine ligand by alkene substrate and direct insertion of alkene double bond into Pd(II)–aryl bond. The rate- and regio-determining step of the catalytic cycle is concerted metalation/deprotonation of arene C–H bond featuring a six-membered ring transition state. Other mechanism alternatives possess much higher activation barriers, and thus are kinetically less competitive. Possible competing homocoupling pathways have also been shown to be kinetically unfavorable. On the basis of the proposed reaction pathway, the regioselectivity predicted for a number of monosubstituted benzenes is in excellent agreement with experimental observations, thus, lending further support for our proposed mechanism. Additionally, the origins of the regioselectivity of C–H bond activation is elucidated to be caused by a major steric repulsion effect of the ancillary pyridine type ligand with ligands on palladium center and a minor electronic effect of the preinstalled substituent on the benzene ring on the cleaving C–H bond. This would finally lead to the formation of a mixture of *meta* and *para* C–H activation products with *meta* products dominating while no *ortho* products were detected. Finally, the multiple roles of the ancillary pyridine type ligand have been discussed. These insights are valuable for our understanding and further development of more efficient and selective transition metal-catalyzed oxidative C–H/C–H coupling reactions.



## 1. INTRODUCTION

Transition metal-catalyzed C–H bond activation reactions have received great attention in recent years and have promising prospects in organic synthesis, material science, pharmaceuticals, and polymer sciences.<sup>1</sup> These reactions exploit the direct functionalization of the C–H bonds of a substrate, excluding the need for prefuctionalization of C–H bonds to other more reactive C–X bonds such as C–halogen bonds as in traditional cross-coupling reactions.<sup>2</sup> Therefore, synthesis utilizing C–H bond activations is more streamlined and atom economic.

Two critical challenges associated with C–H bond activation reactions include the promotion of the reactivity of relatively inert C–H bonds and the control of regioselectivity of C–H activation. As to the reactivity problem, it has been shown that coordination of some transition metals (TM) to a substrate could

promote the cleavage of the C–H bond and subsequent formation of the TM–C bond, which is reactive toward a series of reactions.<sup>1d,j</sup> Consequently, a wide range of transition metals, particularly palladium salts, have been used to develop various transition metal-mediated C–H activation reactions and great progress has been made.

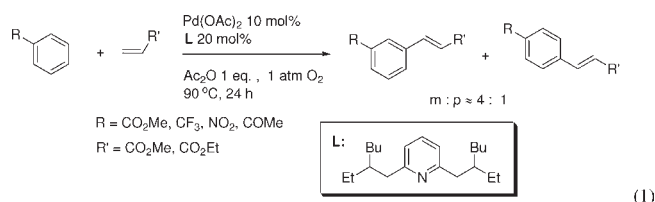
On the other hand, the regioselectivity of the C–H activation reactions presents a more challenging problem. In the context of electrophilic aromatic substitution mechanism, the product mixtures usually contain *ortho*, *meta*, and *para* isomers. Selective functionalization of a specific C–H bond of a substrate is desired for a reaction to be useful for practical applications.

Received: June 10, 2011

Published: November 23, 2011

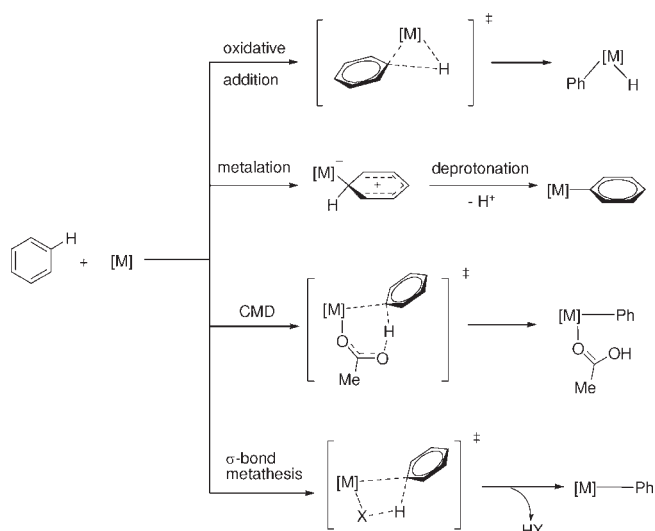
Until now, two general strategies have been used to control selectivity for C–H bond activation of a complex substrate containing multiple C–H bonds. The first is to use the directing effect of a coordinating group of the substrate to deliver the transition metal to the proximity of a specific C–H bond, thus, generating regioselectively the desired product.<sup>3</sup> The well-developed transition metal-catalyzed *ortho*-directed C–H bond activation reactions demonstrate the power of this strategy and have shown great potential in organic synthesis.<sup>1</sup> The other strategy is to exploit the unsymmetrical distribution of electron density on heteroarene ring to accomplish selective activation of specific C–H bonds, such as the more acidic ones.<sup>4</sup>

Despite the advances achieved in directed *ortho* C–H activation reactions, selective *meta* or *para* C–H activations of substituted arenes remain scarce.<sup>5–7</sup> Recently, Gaunt et al. have shown that in the presence of Cu(OTf)<sub>2</sub>, electron-rich anilides can be exclusively arylated at the *meta* position by diaryliodonium salts.<sup>5a</sup> Under similar conditions, *para*-selective C–H arylation products were obtained for some anilines and anisoles derivatives without a directing carbonyl group.<sup>5b</sup> Miyaura and Hartwig et al. have reported the selective *meta*-borylation of arenes using an iridium catalyst.<sup>6</sup> The regioselectivity is believed to be caused by the steric repulsion between the existing groups on the arene ring and ligands on the metal center, rendering the favorable attack of the less hindered *meta* C–H bond.



To achieve selective oxidative coupling of two C–H bonds, Yu et al. recently developed a protocol for the *meta*-selective olefination of *electron-deficient* arenes. In the presence of Pd(OAc)<sub>2</sub> and sterically demanding pyridine type ligands, oxidative coupling of arenes bearing CF<sub>3</sub>, NO<sub>2</sub>, Ac, or CO<sub>2</sub>Me group with electron-deficient alkenes can be achieved (eq 1).<sup>7</sup> It has been shown that the employment of well-designed pyridine type ligands is crucial, which is supposed to effect minimal steric hindrance immediately around the coordinating nitrogen atom but significant steric demand far away. The product regioselectivity is noteworthy where typically a mixture of approximately 4:1 of *meta* to *para* C–H activation products were obtained and no *ortho*-alkenylated products were detected.<sup>7</sup> Yu's reaction represents a conceptually new C–H bond activation reaction, formally an oxidative Heck-type coupling reaction<sup>8,9</sup> exploiting arenes in place of aryl halides as in traditional Heck reactions.<sup>10</sup> It is noteworthy that in Yu's reaction electron-deficient arenes were coupled with alkenes, which is a difficult task. Generally electron-rich arenes have been employed as the substrates in such oxidative Heck couplings<sup>8,9</sup> and other C–H activation reactions such as the Fujiwara reactions,<sup>11</sup> which are believed to promote the critical C–H activation of arenes by transition metal complexes. Additionally, the *meta*-selectivity is significant in view of the fact that some examples have shown that carbonyl or carboxylate are good *ortho*-directing groups in Pd-catalyzed C–H bond activation reactions.<sup>12</sup> As a result, the mechanism of Yu's reaction, especially the factors controlling the regioselectivity of this reaction, greatly intrigued us.

### Scheme 1. Proposed C–H Activation Mechanisms in Transition Metal Catalysis<sup>a</sup>



<sup>a</sup> [M] represents a transition metal complex.

Typically, there are four major kinds of mechanisms for transition metal-mediated C–H bond activation: oxidative addition,<sup>13</sup> traditional electrophilic aromatic substitution,<sup>14</sup> concerted metalation/deprotonation mechanism,<sup>15,16</sup> and  $\sigma$ -bond metathesis mechanism (Scheme 1).<sup>17</sup> Oxidative addition of a C–H bond to low-oxidation state, electron-rich transition metal complexes would lead to the formation of transition metal hydride intermediates. On the contrary, electrophilic aromatic substitution and concerted metalation/deprotonation mechanisms would remove hydrogen atom of the reacting C–H bond in the form of proton. Electrophilic aromatic substitution involves a rate-limiting metalation step, followed by a rapid deprotonation step to rearomatize, thus, generating a TM–aryl intermediate. In contrast, concerted metalation/deprotonation mechanism involves the simultaneous cleavage of the C–H bond and the formation of TM–aryl bond.<sup>18</sup> Finally,  $\sigma$ -bond metathesis mechanism involves a typical four-membered ring transition state composed of TM–X  $\sigma$ -bond and the cleaving C–H  $\sigma$ -bond.

In view of the fundamental importance of Yu's oxidative Heck-type coupling reaction of arenes with alkenes and its interesting yet amazing *meta*-regioselectivity, a detailed study on its mechanism is highly desirable. The following issues are awaiting answers: (1) which C–H activation mechanism is operative for Yu's reaction?; (2) whether activation of arenes precedes activation of alkenes, or a reverse sequence is preferred?; (3) what factors account for the *meta*-selectivity?; (4) what are the roles of the sterically demanding pyridine-type ligand? In this manuscript, systematic studies of two categories of reaction pathways have been done, that is, pathways involving initial arene C–H activation followed by alkene activation and pathways involving initial alkene C–H activation followed by arene activation. For each C–H bond activation step, all possible mechanistic possibilities shown in Scheme 1 as well as other alternatives have been considered. Our results indicate that a pathway featuring an initial CMD mechanism for the arene C–H activation followed by a critical substitution of the pyridine-type ligand by alkene is favored, in which the rate and regioselectivity of the reaction are controlled by the stability of a concerted cyclic transition state.

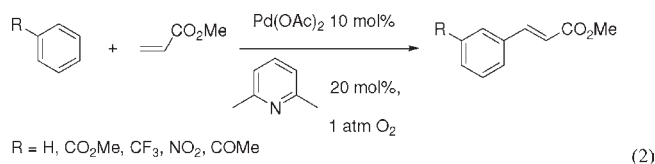
The reason for the regioselectivity and the roles of the pyridine type ligand are discussed. This study represents the first comprehensive theoretical study on the reaction mechanism of such transition metal-catalyzed oxidative C–H/C–H coupling reactions in the literature and presents a detailed full catalytic cycle for a Pd-catalyzed oxidative Heck-type C–H/C–H coupling reaction.<sup>19</sup> We believe that these results are valuable for our understanding and further development of new transition metal-catalyzed regioselective C–H bond activation reactions.

## 2. METHODS AND THEORETICAL MODELS

**2.1. Computational Methods.** All calculations were performed with Gaussian 03.<sup>20</sup> B3LYP method was used.<sup>21</sup> Geometry optimization was conducted with a combined basis set in which Pd was described by LANL2DZ basis set and the effective core potential implemented, and 6-31G(d) was used for the other atoms.<sup>22</sup> Frequency analysis was conducted at the same level of theory to verify the stationary points to be real minima or saddle points and to obtain the thermodynamic energy corrections. For each saddle point, the intrinsic reaction coordinate (IRC) analysis<sup>23</sup> was carried out to confirm that it connected the correct reactant and product on the potential energy surface. Natural population analysis (NPA) was performed also at the same level of theory.<sup>24</sup> Single-point energy calculations were performed on the stationary points by using a larger basis set, that is, SDD<sup>25</sup> for Pd and 6-311+G(d, p) for the other elements. Solvent effect (solvent = benzene) was calculated by using self-consistent reaction field method<sup>26</sup> with CPCM solvation model<sup>27</sup> and UAHF radii.<sup>28</sup> Single-point energies corrected by Gibbs free energy corrections and solvation energies were used to describe the reaction energetics throughout the study. For complexes with several possible isomers, the most stable ones were discussed unless otherwise noted.

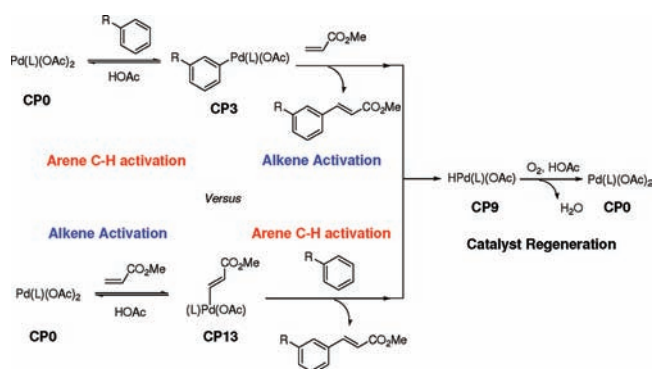
### 2.2. Model Reaction and Overview of Reaction Pathways.

The model reaction is shown in eq 2. For the assessment of various mechanisms shown in Scheme 1, benzene and methyl acrylate were used as the substrates and 2,6-dimethylpyridine was used to model the electronic effect of the original bulkier ligand employed in Yu's reactions. Although the steric effect of the real ligand may not be well represented by this model ligand, this should not affect the relative easiness of different mechanisms. This can be verified by the results that the use of a more bulky and realistic ligand essentially leads to the same conclusions as this model ligand (see Supporting Information for more information). Substituted benzenes were studied in order to evaluate the regioselectivity of the reaction pathway.



Complex **CP0** (Pd(L)(OAc)<sub>2</sub>) with monopyridine ligand is selected as the starting point for the following reasons. First, experimental NMR observations by Yu et al. suggest the release of one molecule of pyridine type ligand from precatalyst containing bis-pyridine type ligands, which is believed to be caused by the mutual repulsion effect of the two congested ligands.<sup>7</sup> Second, calculation results show that dissociation of one molecule of 2,6-dimethylpyridine ligand from L<sub>2</sub>Pd(OAc)<sub>2</sub> to form **CP0** is exothermic by 1.9 kcal/mol. Third, calculation results show that the conversion of dimeric complex [LPd(OAc)<sub>2</sub>]<sub>2</sub> to two molecules of **CP0** is slightly exothermic by 0.9 kcal/mol, and subsequently, the dimeric complex is believed to be in equilibrium with the monomeric form of **CP0**. The dimeric form is coordination-saturated for Pd center,

## Scheme 2. Overview of Pathways for the Pd(II)-Catalyzed Oxidative Heck Coupling<sup>a</sup>



<sup>a</sup> L denotes 2,6-dimethylpyridine throughout this study.

and therefore, the coordination-unsaturated **CP0** is more likely to be the active form to bind the arene substrate and advance the reaction. Finally, the binding free energy of 2,6-dimethylpyridine ligand in **CP0** has been shown to be very high, 39.1 kcal/mol.

Two major kinds of pathways have been envisaged as shown in Scheme 2. They differ only in the sequence of arene activation versus alkene activation. In the first kind of pathways, initial arene C–H activation occurs to get a Pd(II)–aryl intermediate, followed by activation of alkenes by this intermediate to produce the coupling product. In the second kind of mechanisms, alkene C–H activation occurs prior to that of arene C–H activation, generating an alkenylated Pd(II) intermediate which then activates the arene substrate to deliver the coupling product. Finally, a common step of reoxidation of the Pd(II)–hydride catalyst would regenerate the active catalyst **CP0** in the presence of oxygen and acetic acid, and completes the catalytic cycle.

In the following sections, detailed results on both kinds of pathways are presented. For both arene C–H and alkene C–H bond activation, all the possible mechanisms as shown in Scheme 1 as well as some other alternatives were considered.

## 3. RESULTS

**3.1. Sequential Arene C–H Activation/Alkene Activation/Catalyst Regeneration Mechanisms.** **3.1.1. Arene C–H Activation Mechanisms (CP0 → CP3).** Reaction coordinates of oxidative addition, concerted metalation/deprotonation, and  $\sigma$ -bond metathesis mechanisms for benzene C–H activation by complex **CP0** were summarized in Figure 1.<sup>29</sup>

Oxidative addition mechanism involves a concerted three-centered transition state **TS1<sub>oxd</sub>** from preformed  $\pi$ -complex **CP1** to form an arylPd(IV) hydride intermediate **CP2** (Figure 2).<sup>30</sup> Then, this Pd(IV) hydride intermediate undergoes reductive elimination to get a phenyl-Pd(II) intermediate **CP3**. However, calculation results show that the activation barrier for the oxidative addition step is as high as 56.2 kcal/mol (Figure 1), thus, making this mechanism kinetically inhibited. This is possibly due to the electrophilic nature of the Pd(II) center which is deleterious for oxidative addition reaction to occur. The subsequent steps were therefore not considered.

In concerted metalation/deprotonation mechanism, the transition state **TS1<sub>CMD</sub>** for benzene C–H activation features a six-membered ring (Figure 1). The bond lengths of Pd–C<sub>ipso</sub>, C<sub>ipso</sub>–H, and H–O<sub>2</sub> bond are 2.15, 1.35, and 1.29 Å, respectively (Figure 2). Similar transition states have also been proposed for



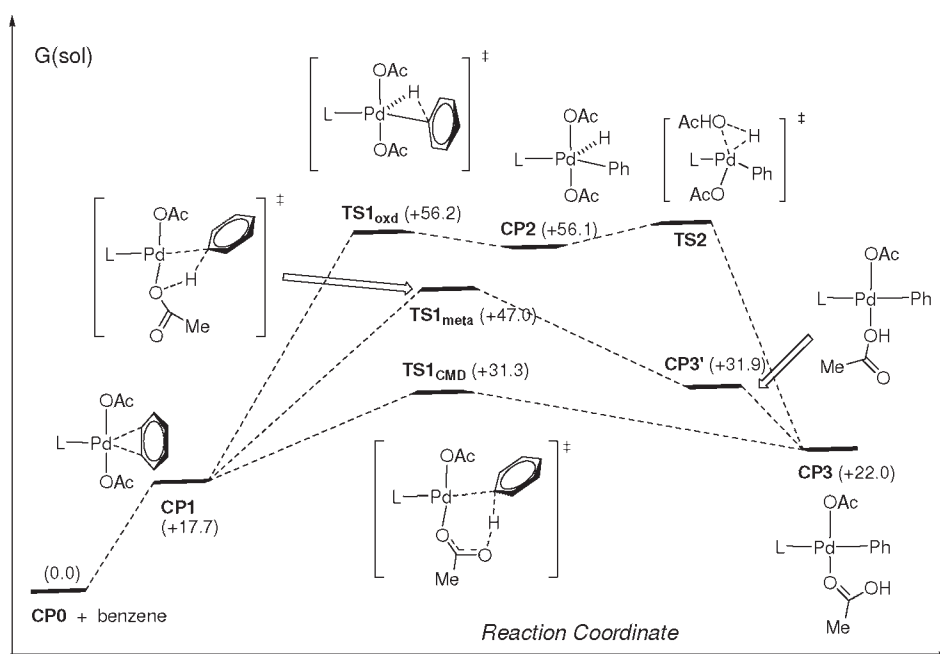


Figure 1. Reaction coordinates for arene C–H activation mechanisms.

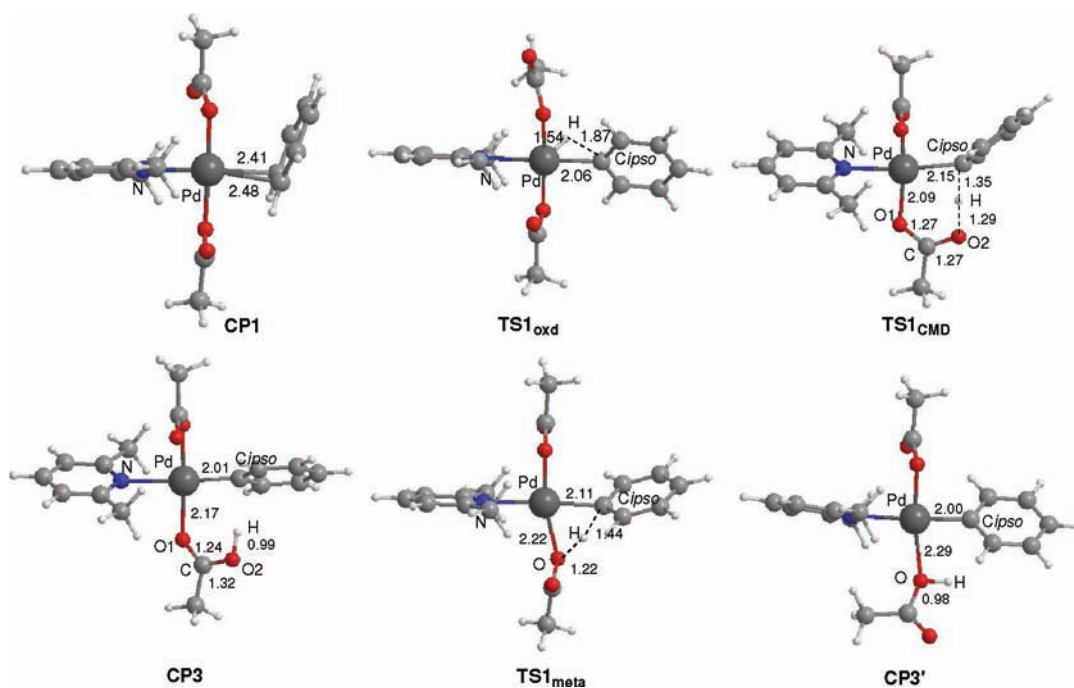


Figure 2. Relevant critical structures involved in oxidative addition, concerted metalation/deprotonation, and  $\sigma$ -bond metathesis mechanisms.

$\text{Pd}(\text{OAc})_2$ -catalyzed direct coupling reactions by Fagnou, Echavarren, and others.<sup>16</sup> In the direct product **CP3**, Pd–*Cipso* and H–O<sub>2</sub> bonds are further shortened to 2.01 and 0.99 Å, respectively, and *Cipso*–H bond is completely broken. All these structural changes indicate the cleavage of the *Cipso*–H bond and the formation of Pd–phenyl bond. **TS1<sub>CMD</sub>** lies about 31.3 kcal/mol above that of the separated reactants **CP0** and benzene.

The  $\sigma$ -bond metathesis transition state **TS1<sub>meta</sub>** contains a distorted four-membered ring composed of Pd–O bond and

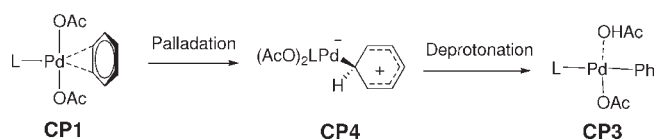
benzene *Cipso*–H bond. The *Cipso*, H, and O atoms are arranged in a nearly linear manner, with bond angle of *Cipso*–H–O being 160.8°. The bond lengths of Pd–*Cipso*, *Cipso*–H, and H–O bond are 2.11, 1.44, and 1.22 Å, respectively. In complex **CP3'**, *Cipso*–H bond is completely broken and Pd–*Cipso* and H–O bonds are further shortened to 2.00 and 0.98 Å, respectively. Unfortunately, the energy level of **TS1<sub>meta</sub>** is too high (47.0 kcal/mol), rendering this  $\sigma$ -bond metathesis mechanism kinetically unfavorable.

We also tried to locate the relevant intermediates in traditional electrophilic aromatic substitution ( $S_{EAr}$ ) mechanism. This mechanism involves initial rate-limiting generation of a palladated intermediate **CP4**, which then undergoes deprotonation to rearomatize to get the Pd(II)–Ph intermediate **CP3** (Scheme 3). Unfortunately, such palladated intermediate **CP4** could not be obtained despite an intensive effort. Geometry optimizations always regenerate to the Pd(II) arene  $\pi$ -complex **CP1**. This implies that the metalated intermediate is unstable on the potential energy surface because the aromaticity is broken at the phenyl ring. Similarly, cationic Pd(II)(OAc)(L) also forms  $\pi$  complex with benzene and the corresponding cationic palladated intermediate could not be obtained. These results indicate that the traditional stepwise metalation/deprotonation mechanism ( $S_{EAr}$ ) is unlikely due to the high instability of the dearomatized intermediate. In contrast, the CMD transition state can effectively delocalize the positive charge accumulated on the benzene ring through polarization of the C–H bond and stabilization of the forming proton atom through binding of oxygen atom of the acetate group.

As can be seen, among all the possible mechanisms examined (Scheme 1 and Figure 1), CMD mechanism with a six-membered ring transition state is the most favorable mechanism for the initial arene C–H bond activation.

**3.1.2. Alkene Activation.** Replacement of the acetic acid ligand or 2,6-dimethylpyridine ligand in complex **CP3** by methyl

**Scheme 3.**  $S_{EAr}$  Mechanism

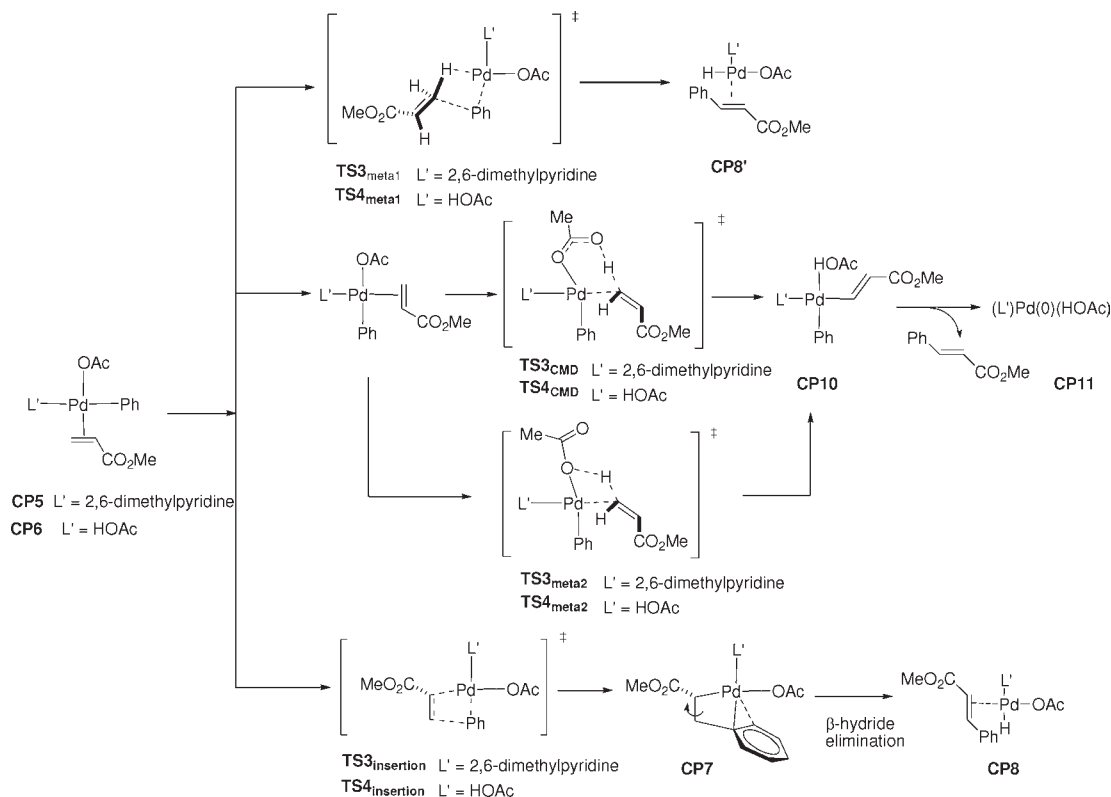


acrylate would give precomplex **CP5** or **CP6** for the subsequent steps. From **CP5** or **CP6**, at least four mechanisms can be conceivable for the alkene activation to get the final coupling product, that is, alkene insertion into Pd–Ph bond, CMD of alkene C–H bond, and metathesis of alkene C–H bond with Pd–Ph or Pd–OAc bond, as shown in Scheme 4.

The first mechanism involves insertion of alkene double bond into Pd(II)–Ph bond, followed by  $\beta$ -hydride elimination to give the coupling product. This mechanism features a typical four-membered ring transition state (Figure 5,  $TS3_{insertion}$  or  $TS4_{insertion}$ ), which is also invoked in the classical Pd-catalyzed Heck reactions of aryl halides with alkenes.<sup>31</sup> The second mechanism for activation of alkene features a second CMD process, to give a Pd(II)(phenyl)(alkenyl) intermediate, which can reductively eliminate the coupling product. The transition state for this process ( $TS3_{CMD}$  or  $TS4_{CMD}$ ) is similar to that of the CMD process for the benzene C–H activation. In the third mechanism, a direct metathesis of alkene C–H bond with Pd(II)–aryl bond via transition state  $TS3_{meta1}$  or  $TS4_{meta1}$  would directly afford the coupling product and a Pd(II)–hydride intermediate. Alternatively, metathesis of alkene C–H bond with Pd–OAc bond via transition state  $TS3_{meta2}$  or  $TS4_{meta2}$  would give intermediate **CP10**, which can reductively eliminate the coupling product. The optimized structures and the relative energies of critical transition states involved in these mechanisms are summarized in Figure 3.

Calculation results show that the relative energies of  $TS3_{insertion}$ ,  $TS3_{CMD}$ ,  $TS3_{meta1}$ , and  $TS3_{meta2}$  are 35.6, 40.0, 60.4, and 51.8 kcal/mol (with  $L' = 2,6$ -dimethylpyridine) and the relative energies of  $TS4_{insertion}$ ,  $TS4_{CMD}$ ,  $TS4_{meta1}$ , and  $TS4_{meta2}$  are 26.0, 42.9, 52.0, and 53.9 kcal/mol (with  $L' = HOAc$ ), respectively. Therefore, for both **CP5** and **CP6**, insertion of alkene

**Scheme 4.** Alkene Activation by Pd(II)–Aryl Intermediate



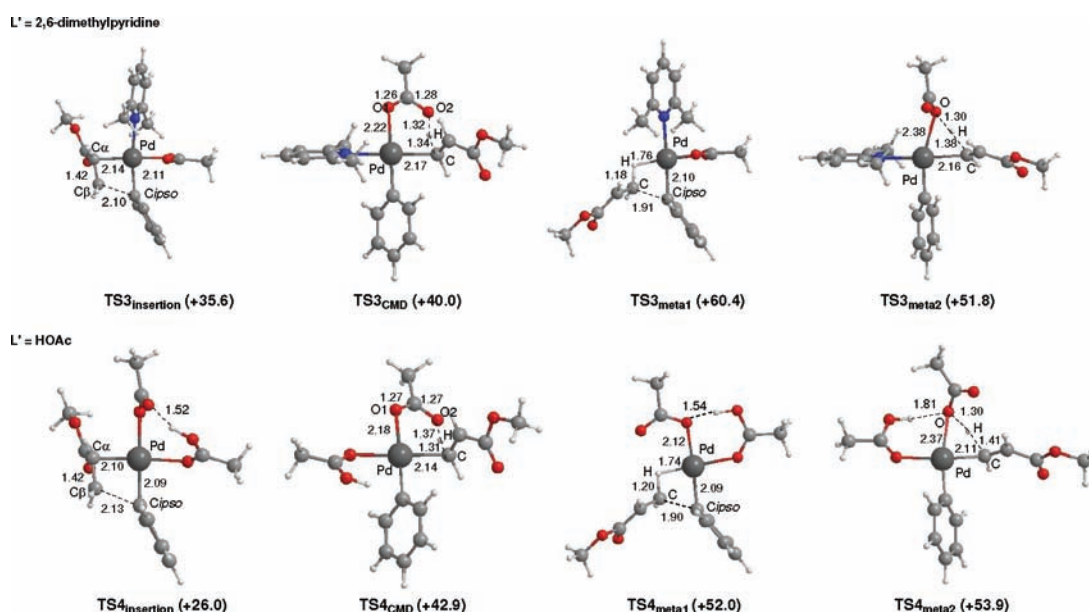


Figure 3. Optimized structures and relative energies of possible transition states for alkene activation.

double bond into Pd(II)–Ph is kinetically the most favorable mechanism and that metathesis and CMD mechanisms are both kinetically inhibited. The most stable transition state is  $TS4_{insertion}$  with  $L' = HOAc$ . Therefore, after arene C–H bond activation to give Pd(II)–aryl intermediate **CP3**, 2,6-dimethylpyridine ligand rather than the in situ formed HOAc in **CP3** is likely to be replaced by the alkene substrate to advance the reaction. Because of the relatively weak binding of 2,6-dimethylpyridine ligand to Pd(II) center, this substitution reaction is thermodynamically favorable, exothermic by 8.1 kcal/mol.

Subsequently, from **CP7**, intramolecular rotation and  $\beta$ -hydride elimination occur readily to give Pd(II)–hydride intermediate **CP8** with coupling product coordinated. This step has an activation energy of only 1.5 kcal/mol while exothermic by 11.1 kcal/mol (for more details about  $\beta$ -hydride elimination, please refer to Supporting Information).

To summarize the results above in section 3.1.2, the most favored mechanism for the activation of alkene should involve insertion of alkene C=C double bond into Pd(II)–Ph bond after the pyridine-type ligand rather than the formed HOAc is replaced by the alkene substrate. Therefore, in the following catalyst regeneration study, only steps following complex **CP8** are considered.

**3.1.3. Catalyst Regeneration.** Complex **CP8** would release the coupling product methyl cinnamate and the left coordination site is occupied by a 2,6-dimethylpyridine ligand, thus, forming Pd(II)–hydride intermediate **CP9**. This ligand substitution process is exothermic by 7.4 kcal/mol. From **CP9**, the active catalyst **CP0** is regenerated. This process has been intensively studied in the literature.<sup>32,33</sup> Generally, two major kinds of mechanisms have been proposed. The first one, called “Pd(0) mechanism”, involves the initial reductive elimination of HOAc from **CP9** and the resulting formation of a Pd(0) species, followed by a reoxidation of this Pd(0) species to Pd(II) active catalyst by oxygen in the presence of HOAc. The second mechanism features a direct insertion of O<sub>2</sub> molecule into the Pd(II)–H bond in **CP9**, generating a Pd(II)–OOH species. Subsequent protonation of this species by HOAc would release

peroxide and regenerate the active catalyst **CP0**. It has been shown that for labile, monodentate ligand, such as pyridine and DMSO, the Pd(0) mechanism is favored.<sup>32,33</sup> Therefore, in this study, we also considered the Pd(0) mechanism.

Reductive elimination of HOAc from **CP9** has an activation barrier of 9.5 kcal/mol and is exothermic by 1.1 kcal/mol. The resulting (HOAc)Pd(0)L is then reoxidized by O<sub>2</sub> in the presence of HOAc to regenerate the active **CP0** complex. This reoxidation process is exothermic by 40.0 kcal/mol. Overall, the catalyst regeneration process from **CP9** to **CP0** is exothermic by 41.1 kcal/mol, indicating that this process is thermodynamically favorable.

Thus, a whole catalytic cycle for the arene activation/alkene activation mechanism is completed. Shown in Figure 4 is the reaction coordinate of kinetically the most favorable pathway involving a sequence of critical CMD activation of arene C–H bond/substitution of pyridine-type ligand by alkene/alkene insertion steps. From Figure 4, it is obvious that the concerted metalation/deprotonation step is the rate-determining step of the catalytic cycle, with a characteristic high-lying six-membered ring transition state. The magnitude of the overall activation barrier (31.3 kcal/mol) is reasonable in view of the fact that the reactions need to be performed at 90 °C for a prolonged time.

**3.2. Alternative Sequential Alkene C–H Activation/Arene Activation Mechanisms.** Pd(OAc)<sub>2</sub> activates alkene C–H bond first, generating a Pd(II)–alkenyl intermediate **CP13** (Scheme 5). Subsequent activation of benzene by this Pd(II)–alkenyl intermediate would give the coupling product. Finally, reoxidation of Pd(II)–hydride intermediate by O<sub>2</sub> would regenerate the active catalyst **CP0**.

**3.2.1. Activation of Alkene C–H Bond by **CP0**.** Activation of alkene C–H bond by complex **CP0** through transition state  $TS7_{CMD}$  or  $TS7_{meta}$  would generate an Pd(II)–alkenyl intermediate **CP13**. The activation barrier for this process is 28.7 kcal/mol for CMD mechanism and 44.8 kcal/mol for metathesis mechanism, while it is endothermic by 16.2 kcal/mol (Scheme 5).<sup>34</sup>

**3.2.2. Activation of Benzene by Pd(II)–Alkenyl.** After substitution of HOAc by benzene forming **CP14** which is endothermic

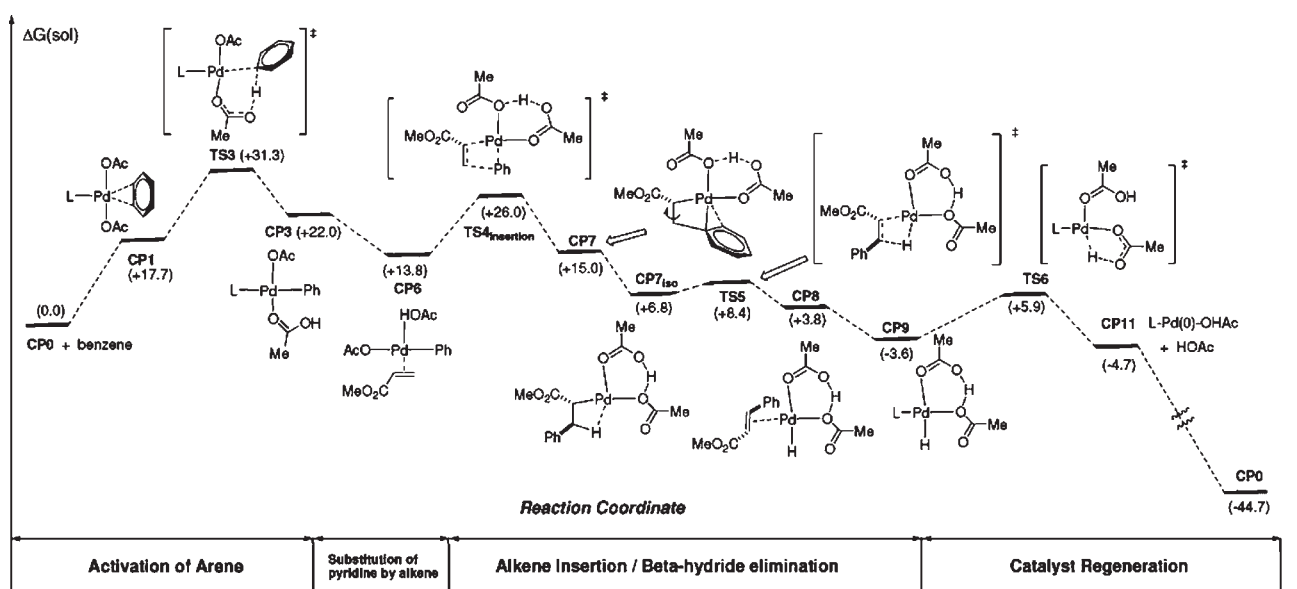
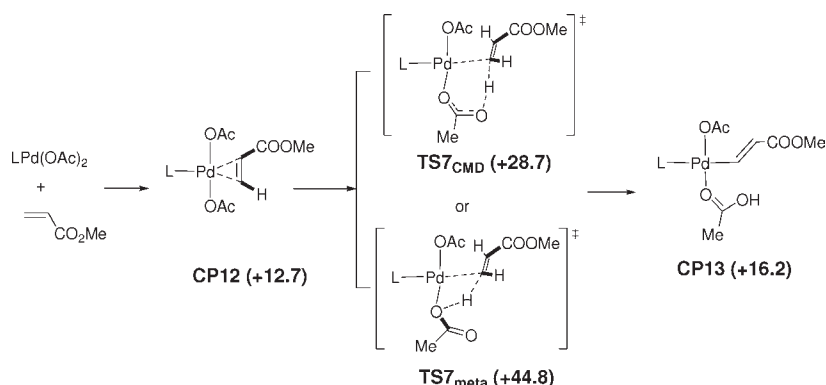


Figure 4. The whole catalytic cycle for sequential arene activation/alkene activation mechanism.

### Scheme 5. Activation of Alkene C–H Bond



by 11.1 kcal/mol, there are several possible mechanisms for the activation of benzene to afford the final coupling product. As shown in Scheme 6, a second CMD of benzene C–H bond, metathesis of benzene C–H bond with Pd–OAc bond or Pd(II)–alkenyl bond and carbopalladation mechanism all can activate the benzene substrate.

Calculation results show that energy levels of these four transition states are 35.1, 47.1, 65.6, and 53.2 kcal/mol for  $TS8_{CMD}$ ,  $TS8_{meta2}$ ,  $TS8_{meta1}$ , and  $TS8_{insertion}$ , respectively. The CMD transition state  $TS8_{CMD}$  is the most stable one among these four transition states. Therefore, the activation of benzene by Pd(II)–alkenyl is likely to follow the CMD mechanism.

We also examined the CMD mechanism in which the pyridine ligand (rather than HOAc) is replaced by benzene before the cleavage of the benzene C–H bond. The energy level of this transition state  $TS9_{CMD}$  is 38.3 kcal/mol, much higher than  $TS8_{CMD}$  by 3.2 kcal/mol (for more information of this mechanism, see Supporting Information). Therefore, it seems that benzene is prone to substitute the HOAc generated to form an intermediate for CMD activation of benzene C–H bond.

The overall pathway for alkene activation/arene activation sequence is summarized in Figure 5. Compared to the overall activation barrier (31.3 kcal/mol) of the favorable pathway in which arene C–H activation precedes the activation of alkene in Figure 4, the pathway involving initial alkene activation followed by arene activation is kinetically less competitive. The difference of the overall activation barrier of 3.8 kcal/mol would make the pathway in Figure 4 dominate overwhelmingly.

**3.3. Possible Competing Homocoupling Pathways.** For the proposed pathway shown in Figure 4, after the generation of CP3, substitution of HOAc or 2,6-dimethylpyridine ligand by a second molecule of benzene and subsequent activation of the second arene substrate should be a possible competing pathway to deliver the arene/arene homocoupling products (Figure 6). However, calculation results show that the overall activation barriers for the second benzene activation is extremely high, 43.0 and 38.3 kcal/mol, respectively. Therefore, arene/arene homocoupling products should be kinetically inhibited.

Similarly, activation of a second alkene by intermediate CP13 would constitute another possible side pathway to form alkene/alkene homocoupling products. Unfortunately, such pathways

## Scheme 6. Activation of Benzene by Pd(II)–Alkenyl Intermediate

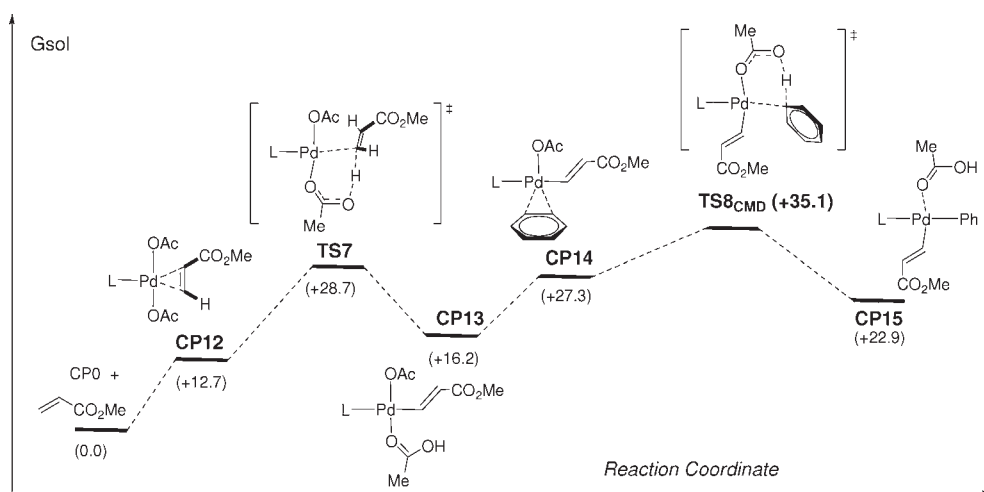
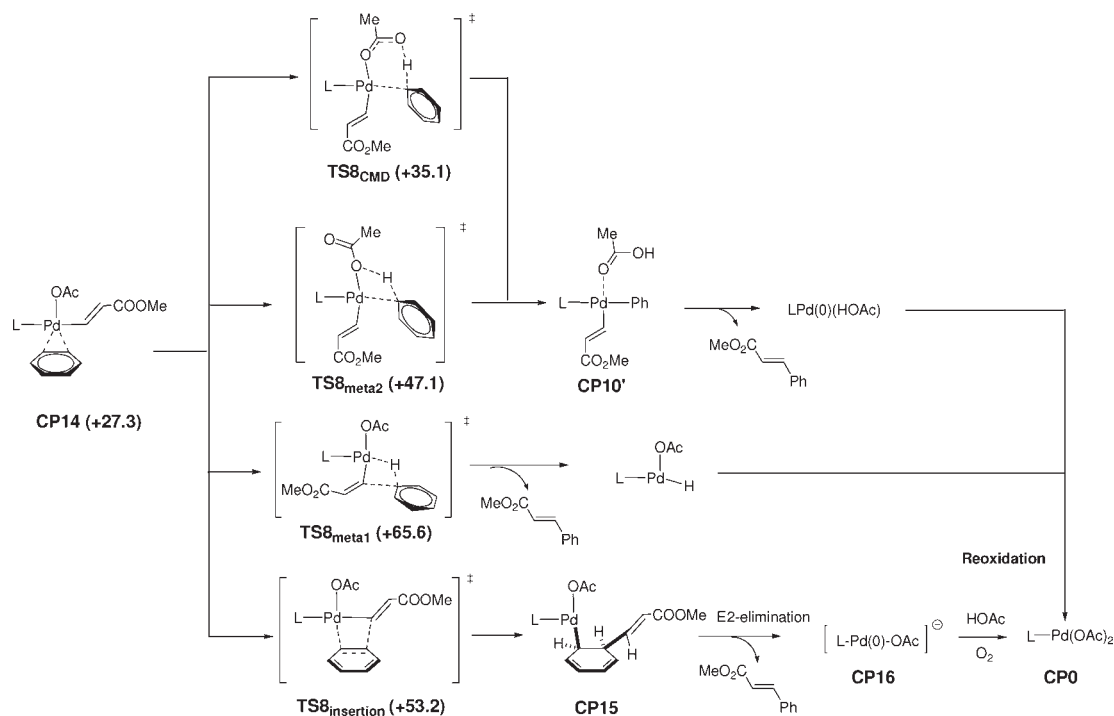


**Figure 5.** The most favored reaction pathway for alkene activation/arene activation sequence (steps following intermediate CP15 were omitted for clarity).

possess also very high activation barriers of 31.8 and 42.5 kcal/mol (see Supporting Information for more information). Considering the fact that the concentration of alkene substrate is 1 to 2 orders of magnitude lower than the arene substrate in Yu's reaction (in most of the reactions, arene substrate were also used as the solvent),<sup>7</sup> the alkene/alkene homocoupling product should also be less significant compared to the desired arene/alkene cross-coupling product.

**3.4. Regioselectivity for the Favored CMD Mechanism for Arene C–H Activation.** To further evaluate the validity of the proposed pathway in Figure 4, the regioselectivity of C–H activation for some monosubstituted benzenes has been examined

under the regio-determining CMD step and the results are summarized in Table 1.

For each substrate, there are five possible transition states  $TS_{ortho}$ ,  $TS_{ortho}'$ ,  $TS_{meta}$ ,  $TS_{meta}'$ , and  $TS_{para}$  for the arene C–H bond cleavage in view of the position of the substituent R on the benzene ring relative to the cleaving C–H bond and the relative stereo orientation of the R substituent and the acetate group, as shown in Table 1. For example, in  $TS_{ortho}$  and  $TS_{ortho}'$ , the substituent R is *ortho* to the cleaving C–H bond. In  $TS_{ortho}$ , the substituent R is *anti* to the acetate group, locating on the opposite side of the palladium coordination plane. However, in  $TS_{ortho}'$ , substituent R and acetate are *syn* to each other. Similar situation



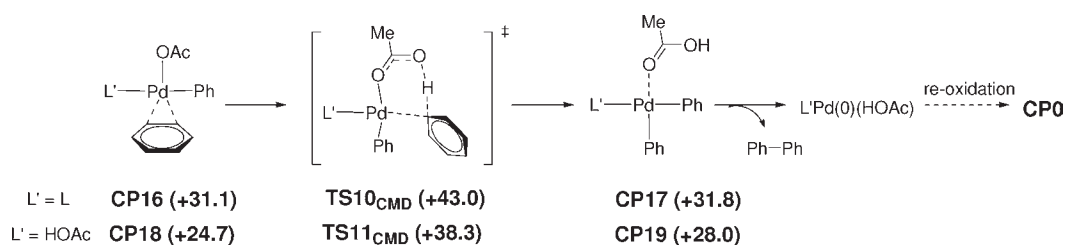
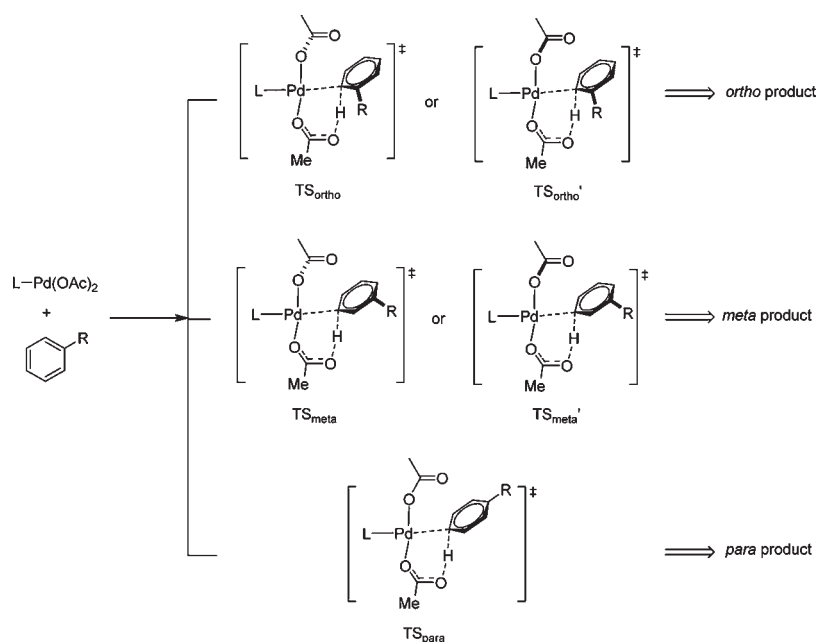


Figure 6. Arene/arene homocoupling side pathway.

Table 1. Relative Energies of the Regio-Determining Transition States for Substituted Benzenes in Concerted Metalation/Deprotonation Mechanism (kcal/mol)<sup>a</sup>

Ph-R (with R =)	TS <sub>ortho</sub>	TS <sub>ortho'</sub>	TS <sub>meta</sub>	TS <sub>meta'</sub>	TS <sub>para</sub>
MeCO	36.3	36.2	31.5	34.3	32.1
CO <sub>2</sub> Me	35.8	36.6	32.1	34.8	32.9
NO <sub>2</sub>	33.4	34.5	30.9	33.3	31.9
CF <sub>3</sub>	34.8	37.0	32.0	34.0	32.0
F	29.6	30.3	32.2	31.7	30.3
Cl	31.5	33.0	31.5	32.4	31.1
Me	31.5	32.2	31.3	31.9	29.5
OMe	30.6	31.9	32.1	32.4	29.2

<sup>a</sup> The structural difference of TS<sub>ortho</sub> and TS<sub>ortho'</sub> is the relative orientations of the acetate group and the R substituent on the benzene ring. Specifically, they are anti to each other compared to the palladium coordination plane in TS<sub>ortho</sub> and syn to each other in TS<sub>ortho'</sub>; Similar designations are for TS<sub>meta</sub> and TS<sub>meta'</sub>. L denotes 2,6-dimethylpyridine ligand.

applies for TS<sub>meta</sub> and TS<sub>meta'</sub>. Note that TS<sub>ortho</sub> and TS<sub>ortho'</sub> would finally lead to the *ortho*-olefination products; TS<sub>meta</sub> and TS<sub>meta'</sub> would finally lead to the *meta*-olefination products; TS<sub>para</sub> would finally give the *para*-olefination products.

Calculation results show that for benzenes with COMe, CO<sub>2</sub>Me, NO<sub>2</sub>, and CF<sub>3</sub> substituents, TS<sub>meta</sub> is the most stable transition state among the five isomers (Table 1). The energy levels of TS<sub>ortho</sub> and TS<sub>ortho'</sub> are substantially higher than TS<sub>meta</sub> and TS<sub>para</sub>, rendering the *ortho*-C–H activation products kinetically unfavorable. Furthermore, TS<sub>meta</sub> is a little more stable

than TS<sub>para</sub> by less than 1.0 kcal/mol.<sup>35</sup> These results would predict that a mixture of *meta*- and *para*-C–H activation products with a major portion of *meta*-C–H activation products should be generated while no *ortho*-C–H activation products could be detected, which is in excellent agreement with Yu's experimental findings.<sup>7</sup>

Additionally, as a comparison, the regioselectivity for substituted benzenes Ph-R with R = F, Cl, Me, and OMe has also been examined under the CMD mechanism although these substrates were not studied in Yu's reaction. Interestingly, *ortho* and/or

*para* C–H activation products are predicted to be dominant for these substrates. This is in line with some experimental observations for related oxidative Heck coupling of toluene, chlorobenzene, and anisole with alkenes.<sup>36–38</sup> For instance, Ishii et al. reported that the coupling of toluene and anisole with cyanide-substituted alkenes led to a mixture of *ortho*-, *meta*-, and *para*-olefination products with *para*-olefination products a little favored; the coupling of chlorobenzene would lead to an *ortho*-, *meta*-, and *para*-product ratio of 35:30:35.<sup>36</sup> Similar results for oxidative coupling of chlorobenzene and anisole with alkenes were reported by Shue and Jacobs et al.<sup>37,38</sup> Noteworthy, the results for fluorobenzene show that *ortho*-C–H activation is favored, which is consistent with reports by Echavarren and Fagnou et al. that fluorinated benzenes indeed prefer activation of C–H bonds that are *ortho* to one or more fluorine atoms on the benzene ring.<sup>16b,d,e</sup>

To summarize, the product regioselectivity predicted on the basis of our proposed pathway is well consistent with experimental observations, thus, lending further support for the validity of the proposed CMD mechanism. Additionally, our results demonstrate that the regioselectivity of C–H activation under the CMD mechanism is sensitive to the electronic properties of the substrates in question. All *ortho*, *meta*, and *para* selectivity can possibly be achieved through altering the substituent on the substrate benzene ring.

## 4. DISCUSSIONS

**4.1. Favorable Reaction Sequence and C–H Activation Mechanism.** To summarize the results in Sections 3.1 and 3.2, a reaction pathway involving a sequence of arene C–H activation/alkene activation (Figure 4) has been supported against the alternative pathway involving a reverse sequence of alkene activation/arene activation. The results indicate that the activation of arene C–H bond should be more difficult than the alkene substrates, and thus, activation of arene constitutes the rate-determining step of both catalytic cycles. Furthermore, among all the possible mechanisms proposed, the most favorable one for arene C–H activation should be the concerted metalation/deprotonation mechanism. The rate-determining step of the arene activation/alkene activation pathway is proposed to involve CMD activation of arene C–H bond by electrophilic (L)Pd(OAc)<sub>2</sub> active catalyst, while in the rate-determining step of the alkene activation/arene activation pathway, the active species to activate arene C–H bond is a less electrophilic (L)(OAc)Pd(II)-alkenyl intermediate. This possibly accounts for the higher activation barrier of the alkene activation/arene activation pathway. In the CMD transition state (TS<sub>1</sub><sup>CMD</sup>) for the arene C–H bond cleavage, acetate anion ligand plays a critical role for the stabilization of the transition state, acting as an electron shuttle between the Pd center and the arene substrate. Such carboxylate effect for transition metal-catalyzed C–H activation reactions has been increasingly recognized.<sup>39</sup>

Possible homocoupling side pathways have also been examined and the results indicate that the activation barriers are higher than that for our proposed pathway (Figure 4). Therefore, the homocoupling products should be unfavorable kinetically. Additionally, the regioselectivity of C–H bond activation predicted for some monosubstituted substrates on the basis of our proposed pathway is generally in good agreement with experimental observations. These additional studies on chemo- and regioselectivity lend further support for the validity of our proposed pathway.

## 4.2. Origins of the *meta*-Regioselectivity for Yu's Reaction.

From the results in columns 2 and 6 of Table 1, for substrates Ph-R (R = MeCO, CO<sub>2</sub>Me, NO<sub>2</sub>, and CF<sub>3</sub>), TS<sub>para</sub> is consistently much more stable than TS<sub>ortho</sub> by 1.5–4.2 kcal/mol. Since the electronic properties of *ortho*- and *para*-position of a substituent on the benzene ring are believed to be similar, the large energy differences between TS<sub>para</sub> and TS<sub>ortho</sub> highlight the significant steric repulsion effect of the preinstalled substituent on the C–H activation step. Therefore, steric effect should be the major reason that *ortho*-olefination product cannot be obtained in the reaction investigated.

On the other hand, a comparison of the relative energies of the TS<sub>meta</sub> and TS<sub>para</sub> for substrates Ph-R with R = MeCO, CO<sub>2</sub>Me, NO<sub>2</sub>, and CF<sub>3</sub> demonstrates that the relatively less electron-deficient *meta* position is slightly preferred for the C–H activation step. For both *meta* and *para* positions, there should be no significant steric effect because the substituent R is far away from the palladium center. This indicates that the *meta* versus *para* selectivity in Yu' reaction should arise from a minor electronic effect and electron-rich C–H bond should be somewhat preferred. This assertion has been supported by the results for monosubstituted benzenes Ph-R with R = F, Cl, Me, and OMe wherein C–H activation preferentially occurs at more electron-rich *ortho/para* C–H positions, and can further be rationalized in view of the frontier orbitals of the CMD transition state wherein only a little contribution comes from the p orbital of the carbon atom of the cleaving C–H bond (see Supporting Information for more information).

In summary, for this Pd-catalyzed oxidative coupling reaction, steric effect should dominate while electronic effect plays a minor role in the regio-determining step. The *ortho*-C–H activation is kinetically unfavorable due to the steric repulsion effect between the preinstalled substituent and ligands on palladium center. The dominant formation of *meta*-C–H activation products versus the *para*-C–H activation products is suggested to be a minor electronic effect of the preinstalled substituent.

**4.3. The Roles of Pyridine Type Ligand.** The roles of the pyridine-type ligand in the oxidative coupling reaction are at least four-fold. First, due to its large steric demand, monopyridine ligated Pd(II) catalyst is formed initially, which can readily combine the arene substrates. Second, the relatively less electron-rich character of pyridine type ligand makes the Pd center more electrophilic, which is beneficial for binding and activating of the arene substrate to effect C–H bond cleavage.<sup>40</sup> Third, after the cleavage of arene C–H bond, it is proposed that the labile nature of the pyridine ligand promotes the replacement of itself by the alkene substrate to advance the reaction. This substitution process would otherwise be difficult for other more electron-rich ancillary ligands such as phosphines or carbenes. Finally, pyridine type ligand promotes the release of the coupling product and the recovery of the active catalyst.

As can be seen, the pyridine type ligand plays multiple roles in almost each step of the catalytic cycle of this Pd-catalyzed oxidative Heck reaction. This may be suggestive and helpful for developing other related transition metal-catalyzed oxidative C–H/C–H coupling reactions.

## 5. CONCLUSIONS

In this paper, a systematic theoretical study on the reaction pathways of Pd(II)-catalyzed oxidative C–H/C–H coupling reaction between electron-deficient arenes and olefins has been

presented for the first time. The following conclusions have been drawn:

- 1 Systematic evaluations of two kinds of reaction mechanisms with the reverse sequence of arene activation versus alkene activation were performed. For both arene activation and alkene activation, several probable mechanisms have been considered, including oxidative addition,  $\sigma$ -bond metathesis, electrophilic aromatic substitution, concerted metalation/deprotonation, and insertion (carbopalladation) mechanisms. Our results strongly favor a reaction pathway involving an initial concerted metalation/deprotonation mechanism for the arene C–H activation, followed by substitution of the pyridine ancillary ligand by the alkene substrate and subsequent activation of the alkene through insertion of alkene double bond into the Pd(II)–aryl bond. The rate- and regio-determining step of this pathway is a common CMD activation of arene C–H bond step featuring a six-membered ring transition state, to form a Pd(II)–aryl intermediate. Possible arene/arene or alkene/alkene homocoupling pathways have been shown to be kinetically less competitive compared to the desired cross-coupling pathway.
- 2 On the basis of the proposed mechanism, product regioselectivity examinations of a number of monosubstituted benzenes Ph-R with R = COMe, CO<sub>2</sub>Me, NO<sub>2</sub>, and CF<sub>3</sub> are in excellent agreement with the experimental findings that a mixture of meta and para C–H activation products were obtained while no ortho-products were detected. Our results indicate that the absence of ortho-C–H activation product is caused by the steric repulsion effect of the preinstalled ortho-substituent with ligands bound on Pd center while the dominant formation of meta-C–H activation products versus para-products is due to a minor electronic effect of the substituent on the cleaving C–H bond. Additionally, examinations of other substituted benzenes Ph-R with R = F, Cl, Me, and OMe demonstrate that the regioselectivity of C–H activation under the proposed CMD mechanism is sensitive to the electronic properties of substrates in question.
- 3 The roles of ancillary pyridine type ligand are at least four-fold deduced from our proposed reaction pathway and empirical experimental findings. First, its large steric demand leads to the formation of monopyridine ligated Pd(II) active catalyst, which readily combines the arene substrate to advance the reaction, excluding the otherwise difficult dissociation of one molecule of ancillary ligand as for other ligands such as phosphines. Second, its relatively weak electron-donating ability makes the Pd center more electrophilic, which is beneficial for the arene C–H activation step. Third, after arene C–H activation step, the pyridine ligand is proposed to be readily replaced by the alkene substrate to continue the reaction. Finally, it promotes the regeneration of the active catalyst during the oxidation of Pd(II)–hydride intermediates by external oxidants.

We believe the results presented in this paper are helpful for the understanding of palladium as well as other transition metals catalyzed oxidative coupling of two C–H partners and should stimulate more studies directed toward development and application of transition metal-catalyzed C–H activation reactions.

## ■ ASSOCIATED CONTENT

**S Supporting Information.** Detailed optimized geometries, free energies, thermal corrections; complete ref 20. This material is available free of charge via the Internet at <http://pubs.acs.org>.

## ■ AUTHOR INFORMATION

### Corresponding Author

slzhang@jiangnan.edu.cn

## ■ ACKNOWLEDGMENT

This study was supported by the National Natural Science Foundation of China (Grant No. 20971058) and the Fundamental Research Funds for the Central Universities (JUSRP 11105). We are grateful to Prof. Lei Liu from Tsinghua University for helpful discussions and suggestions during our preparation of this manuscript.

## ■ REFERENCES

- (1) For recent reviews on transition metal-catalyzed C–H activation reactions, see: (a) Ritleng, V.; Sirlin, C.; Pfeffer, M. *Chem. Rev.* **2002**, *102*, 1731. (b) Campeau, L.-C.; Fagnou, K. *Chem. Commun.* **2006**, 1253. (c) Godula, K.; Sames, D. *Science* **2006**, *312*, 67. (d) Alberico, D.; Scott, M. E.; Lautens, M. *Chem. Rev.* **2007**, *107*, 174. (e) Seregin, I. V.; Gevorgyan, V. *Chem. Soc. Rev.* **2007**, *36*, 1173. (f) Davies, H. M. L.; Manning, J. R. *Nature* **2008**, *451*, 417. (g) Chen, X.; Engle, K. M.; Wang, D. H.; Yu, J.-Q. *Angew. Chem., Int. Ed.* **2009**, *48*, 5094. (h) Daugulis, O.; Do, H.-Q.; Shabashov, D. *Acc. Chem. Res.* **2009**, *42*, 1074. (i) Ackermann, L.; Vicente, R.; Kapdi, A. R. *Angew. Chem., Int. Ed.* **2009**, *48*, 9792. (j) Lyons, T. W.; Sanford, M. S. *Chem. Rev.* **2010**, *110*, 1147.
- (2) For a general review on classical transition metal-catalyzed cross-coupling reactions, see: *Metal-Catalyzed Cross-Coupling Reactions*; de Meijere, A.; Diederich, F., Eds.; Wiley: Weinheim, Germany, 2004.
- (3) For directing group effects, see: (a) Li, B.-J.; Yang, S.-D.; Shi, Z.-J. *Synlett* **2008**, 949. (b) Yu, J.-Q.; Giri, R.; Chen, X. *Org. Biomol. Chem.* **2006**, *4*, 4041.
- (4) For heteroarene electronic effect: (a) Do, H.-Q.; Daugulis, O. *J. Am. Chem. Soc.* **2007**, *129*, 12404. (b) Kirchberg, S.; Tani, S.; Ueda, K.; Yamaguchi, J.; Studer, A.; Itami, K. *Angew. Chem., Int. Ed.* **2011**, *50*, 2387. (c) Kim, M.; Kwak, J.; Chang, S. *Angew. Chem., Int. Ed.* **2009**, *48*, 8935. (d) Turner, G. L.; Morris, J. A.; Greaney, M. F. *Angew. Chem., Int. Ed.* **2007**, *46*, 7996.
- (5) (a) Phipps, R. J.; Gaunt, M. J. *Science* **2009**, *323*, 1593. (b) Tredwell, M. J.; Gulias, M.; Bremeyer, N. G.; Johansson, C. C. C.; Collins, B. S. L.; Gaunt, M. J. *Angew. Chem., Int. Ed.* **2011**, *50*, 1076. (c) Zhou, Y.; Zhao, J.; Liu, L. *Angew. Chem., Int. Ed.* **2009**, *48*, 7126.
- (6) Ishiyama, T.; Takagi, J.; Ishida, K.; Miyaura, N.; Anastasi, N. R.; Hartwig, J. F. *J. Am. Chem. Soc.* **2002**, *124*, 390.
- (7) Zhang, Y.-H.; Shi, B.-F.; Yu, J.-Q. *J. Am. Chem. Soc.* **2009**, *131*, 5072.
- (8) For a recent review on oxidative Heck coupling reactions, see: Bras, J. L.; Muzart, J. *Chem. Rev.* **2011**, *111*, 1170.
- (9) For Pd-catalyzed ortho-directed olefination of arenes or heteroarenes, see: (a) Boele, M. D. K.; van Strijdonck, G. T. P. F.; de Vries, A. H. M.; Kamer, P. C. J.; de Vries, J. G.; van Leeuwen, P. W. N. M. *J. Am. Chem. Soc.* **2002**, *124*, 1586. (b) Wang, J.-R.; Yang, C.-T.; Liu, L.; Guo, Q.-X. *Tetrahedron Lett.* **2007**, *48*, 5449. (c) Zaitsev, V. G.; Daugulis, O. *J. Am. Chem. Soc.* **2005**, *127*, 4156. (d) Cai, G.; Fu, Y.; Li, Y.; Wan, X.; Shi, Z. *J. Am. Chem. Soc.* **2007**, *129*, 7666. (e) Li, J.-J.; Mei, T.-S.; Yu, J.-Q. *Angew. Chem., Int. Ed.* **2008**, *47*, 6452. (f) Cho, S. H.; Hwang, S. J.; Chang, S. *J. Am. Chem. Soc.* **2008**, *130*, 9254. (g) Lu, Y.; Wang, D.-H.; Engle, K. M.; Yu, J.-Q. *J. Am. Chem. Soc.* **2010**, *132*, 5916. (h) Engle, K. M.; Wang, D.-H.; Yu, J.-Q. *Angew. Chem., Int. Ed.* **2010**, *49*, 6169. (i) Grimster, N. P.; Gauntlett, C.; Godfrey, C. R. A.; Gaunt, M. J. *Angew. Chem., Int. Ed.* **2005**, *44*, 3125. (j) Yokota, T.; Tani, M.; Sakaguchi, S.; Ishii, Y. *J. Am. Chem. Soc.* **2003**, *125*, 1476. (k) Dams, M.; De Vos, D. E.; Celen, S.; Jacobs, P. A. *Angew. Chem., Int. Ed.* **2003**, *42*, 3512.
- (10) For recent reviews on Heck reactions, see: (a) Beletskaya, I. P.; Cheprakov, A. V. *Chem. Rev.* **2000**, *100*, 3009. (b) Dounay, A. B.; Overman, L. E. *Chem. Rev.* **2003**, *103*, 2945.



- (11) (a) Moritani, I.; Fujiwara, Y. *Tetrahedron Lett.* **1967**, *8*, 1119. (b) Jia, C.; Piao, D.; Oyamada, J.; Lu, W.; Kitamura, T.; Fujiwara, Y. *Science* **2000**, *287*, 1992.
- (12) For carbonyl, carboxylate or amide as directing groups: (a) ref 3a. (b) Wang, D.-H.; Engle, K. M.; Shi, B.-F.; Yu, J.-Q. *Science* **2010**, *327*, 315. (c) Shi, B.-F.; Zhang, Y.-H.; Lam, J. K.; Wang, D.-H.; Yu, J.-Q. *J. Am. Chem. Soc.* **2010**, *132*, 460. (d) Zhang, Y.-H.; Yu, J.-Q. *J. Am. Chem. Soc.* **2009**, *131*, 14654. (e) Xiao, B.; Fu, Y.; Xu, J.; Gong, T. J.; Dai, J.-J.; Yi, Y.; Liu, L. *J. Am. Chem. Soc.* **2010**, *132*, 468. (f) Xiao, B.; Gong, T.-J.; Xu, J.; Liu, Z.-J.; Liu, L. *J. Am. Chem. Soc.* **2011**, *133*, 1466.
- (13) For proposals of C–H oxidative addition mechanisms, see: (a) Mota, A. J.; Dedieu, A.; Bour, C.; Suffert, J. *J. Am. Chem. Soc.* **2005**, *127*, 7171. (b) Campo, M. A.; Huang, Q.; Yao, T.; Tian, Q.; Larock, R. C. *J. Am. Chem. Soc.* **2003**, *125*, 11506. (c) Capito, E.; Brown, J. M.; Ricci, A. *Chem. Commun.* **2005**, 1854.
- (14) For proposals of traditional  $S_EAr$  mechanism, see: (a) Catellani, M.; Chiusoli, G. P. *J. Organomet. Chem.* **1992**, *425*, 151. (b) Hughes, C. C.; Trauner, D. *Angew. Chem., Int. Ed.* **2002**, *41*, 1569. (c) Hennessy, E. J.; Buchwald, S. L. *J. Am. Chem. Soc.* **2003**, *125*, 12084. (d) Park, C.-H.; Ryabova, V.; Seregin, I. V.; Sromek, A. W.; Gevorgyan, V. *Org. Lett.* **2004**, *6*, 1159. (e) Lane, B. S.; Brown, M. A.; Sames, D. *J. Am. Chem. Soc.* **2005**, *127*, 8050.
- (15) For early proposals of concerted metalation/deprotonation mechanism, see: (a) Sokolov, V. I.; Troitskaya, L. L.; Reutov, O. A. *J. Organomet. Chem.* **1979**, *182*, 537. (b) Ryabov, A. D.; Sakodinskaya, I. K.; Yatsimirsky, A. K. *Dalton Trans.* **1985**, 2629. (c) Biswas, B.; Sugimoto, M.; Sakaki, S. *Organometallics* **2000**, *19*, 3895.
- (16) For some recent theoretical or combined experimental/theoretical studies concerning Pd-mediated concerted metalation/deprotonation of arene C–H bond, see: (a) Davies, D. L.; Donald, S. M. A.; Macgregor, S. A. *J. Am. Chem. Soc.* **2005**, *127*, 13754. (b) García-Cuadrado, D.; Braga, A. A. C.; Maseras, F.; Echavarren, A. M. *J. Am. Chem. Soc.* **2006**, *128*, 1066. (c) Lafrance, M.; Fagnou, K. *J. Am. Chem. Soc.* **2006**, *128*, 16496. (d) Lafrance, M.; Rowley, C. N.; Woo, T. K.; Fagnou, K. *J. Am. Chem. Soc.* **2006**, *128*, 8754. (e) García-Cuadrado, D.; de Mendoza, P.; Braga, A. A. C.; Maseras, F.; Echavarren, A. M. *J. Am. Chem. Soc.* **2007**, *129*, 6880. (f) Gorelsky, S. I.; Lapointe, D.; Fagnou, K. *J. Am. Chem. Soc.* **2008**, *130*, 10848.
- (17) For  $\sigma$ -bond metathesis mechanism, see: (a) Hennessy, E. J.; Buchwald, S. L. *J. Am. Chem. Soc.* **2003**, *125*, 12084. (b) Mota, A. J.; Dedieu, A.; Bour, C.; Suffert, J. *J. Am. Chem. Soc.* **2005**, *127*, 7171. (c) Go'mez, M.; Granell, J.; Martinez, M. *Organometallics* **1997**, *16*, 2539. (d) Go'mez, M.; Granell, J.; Martinez, M. *J. Chem. Soc., Dalton Trans.* **1998**, 37.
- (18) In some literature,  $S_EAr$  and the CMD mechanisms are regarded as the same. However, in our study, they are distinguished from each other.
- (19) Although some theoretical studies have appeared in the literature concerning C–H activation mechanisms, there has been no example of such detailed systematic study on the whole catalytic cycles and the regioselectivity origins for transition metal-catalyzed oxidative C–H/C–H coupling reactions.
- (20) Frisch, M. J.; Trucks, G. W.; Schlegel, H. B.; et al. *Gaussian 03, Revision D.01*; Gaussian, Inc.: Wallingford, CT, 2004.
- (21) Becke, A. D. *J. Chem. Phys.* **1993**, *98*, 5648.
- (22) Hay, P. J.; Wadt, W. R. *J. Chem. Phys.* **1985**, *82*, 299.
- (23) Gonzalez, C.; Schlegel, H. B. *J. Phys. Chem.* **1990**, *94*, 5523.
- (24) (a) Reed, A. E.; Weinstock, R. B.; Weinhold, F. *J. Chem. Phys.* **1985**, *83*, 735. (b) Glendening, E. D.; Reed, A. E.; Carpenter, J. E.; Weinhold, F. *NBO Version 3.1 in the Gaussian 98 Package*; University of Wisconsin: Madison, WI, 1990.
- (25) Dolg, M.; Wedig, U.; Stoll, H.; Preuss, H. *J. Chem. Phys.* **1987**, *86*, 866.
- (26) Cossi, M.; Rega, N.; Scalmani, G.; Barone, V. *J. Comput. Chem.* **2003**, *24*, 669.
- (27) (a) Tomasi, J.; Mennucci, B.; Cammi, R. *Chem. Rev.* **2005**, *105*, 2999. (b) Fu, Y.; Liu, L.; Li, R.-Q.; Liu, R.; Guo, Q.-X. *J. Am. Chem. Soc.* **2004**, *126*, 814.
- (28) We also examined other radii for the CPCM calculations of the solvation energies such as Bondi and UFF, and they essentially give the same conclusions. Please refer to Supporting Information for more detailed information.
- (29) All the transition states have an isomeric, less stable geometry with pyridine type ligand cis to the benzene substrate. Please refer to Supporting Information for detailed information.
- (30) For examples of the synthesis and reactivity of Pd(IV) complexes, see: (a) Whitfield, S. R.; Sanford, M. S. *J. Am. Chem. Soc.* **2007**, *129*, 15142. (b) Fu, Y.; Li, Z.; Liang, S.; Guo, Q.-X.; Liu, L. *Organometallics* **2008**, *27*, 3736. (c) Racowski, J. A.; Dick, A. R.; Sanford, M. S. *J. Am. Chem. Soc.* **2009**, *131*, 10974. (d) Ball, N. D.; Sanford, M. S. *J. Am. Chem. Soc.* **2009**, *131*, 3796. (e) Furuya, T.; Benitez, D.; Tkatchouk, E.; Strom, A. E.; Tang, P.; Goddard, W. A.; Ritter, T. *J. Am. Chem. Soc.* **2010**, *132*, 3793.
- (31) (a) Lin, B.-L.; Liu, L.; Fu, Y.; Luo, S.-W.; Chen, Q.; Guo, Q.-X. *Organometallics* **2004**, *23*, 2114. (b) Cui, X.; Li, Z.; Tao, C.-Z.; Xu, Y.; Li, J.; Liu, L.; Guo, Q.-X. *Org. Lett.* **2006**, *8*, 2467.
- (32) For oxidation of the hydride-Pd(II) intermediate, see: (a) Stahl, S. S. *Angew. Chem., Int. Ed.* **2004**, *43*, 3400. (b) Gligorich, K. M.; Sigman, M. S. *Angew. Chem., Int. Ed.* **2006**, *45*, 6612. (c) Piera, J.; Backvall, J.-E. *Angew. Chem., Int. Ed.* **2008**, *47*, 3506.
- (33) For some recent studies related to this subject, see: (a) Landis, C. R.; Morales, C. M.; Stahl, S. S. *J. Am. Chem. Soc.* **2004**, *126*, 16302. (b) Popp, B. V.; Stahl, S. S. *J. Am. Chem. Soc.* **2007**, *129*, 4410. (c) Konnick, M. M.; Stahl, S. S. *J. Am. Chem. Soc.* **2008**, *130*, 5753. (d) Keith, J. M.; Goddard, W. A., *J. Am. Chem. Soc.* **2009**, *131*, 1416. (e) Popp, B. V.; Stahl, S. S. *Chem.—Eur. J.* **2009**, *15*, 2915. (f) Zhang, S.-L.; Fu, Y.; Shang, R.; Guo, Q.-X.; Liu, L. *J. Am. Chem. Soc.* **2010**, *132*, 638. (g) Shang, R.; Xu, Q.; Jiang, Y.-Y.; Wang, Y.; Liu, L. *Org. Lett.* **2010**, *12*, 1000.
- (34) Transition states for oxidative addition and  $S_EAr$  mechanisms for alkene activation by complex CP0 were also examined, but could not be obtained. However, these transition states are expected to be very unstable when analogous with activation of benzene by complex CP0, because it should be difficult for electrophilic CP0 to activate electron-deficient alkenes.
- (35) Although the results for the CF<sub>3</sub> case are not so good, it should be caused by the calculation accuracy problem (possibly due to the errors from estimation of solvation energies) in view of the facts that the error bars for the estimation of solvation energies for current solvation models in most computational packages are often around several kcal/mol and the energy differences in our system are generally less than 1.0 kcal/mol. Furthermore, it is necessary to point out that the calculated gas-phase free energy of TS<sub>meta</sub> is actually 0.3 kcal/mol lower than TS<sub>para</sub> and the gas-phase enthalpy of TS<sub>meta</sub> is 0.8 kcal/mol lower than TS<sub>para</sub> for the CF<sub>3</sub> case.
- (36) Obora, Y.; Okabe, Y.; Ishii, Y. *Org. Biomol. Chem.* **2010**, *8*, 4071.
- (37) (a) Shue, R. S. *Chem. Commun.* **1971**, 1510. (b) Shue, R. S. *J. Catal.* **1972**, *26*, 112.
- (38) Dams, M.; De Vos, D. E.; Celen, S.; Jacobs, P. A. *Angew. Chem., Int. Ed.* **2003**, *42*, 3512.
- (39) Ackermann, L. *Chem. Rev.* **2011**, *111*, 1315.
- (40) Tan, Y.; Hartwig, J. F. *J. Am. Chem. Soc.* **2011**, *133*, 3308.